Available online at www.sciencedirect.com
SCIENCE DIRECT
Journal of Catalysis 231 (2005) 139–150
JOURNAL OF CATALYSIS
www.elsevier.com/locate/jcat

Influence of co-metals on bimetallic palladium catalysts for methane combustion

K. Persson [a,*], A. Ersson [a], K. Jansson [b], N. Iverlund [a], S. Järås [a]

[a] *Department of Chemical Engineering and Technology, KTH, Chemical Technology, Teknikringen 42, SE-100 44, Stockholm, Sweden*
[b] *Arrhenius Laboratory, Department of Inorganic Chemistry, University of Stockholm, S. Arrhenius väg 12, SE-106 91 Stockholm, Sweden*

Received 27 October 2004; revised 5 January 2005; accepted 11 January 2005

Abstract

The catalytic combustion of methane has been investigated over eight different bimetallic palladium catalysts, comprising the co-metals Co, Rh, Ir, Ni, Pt, Cu, Ag, or Au. The catalysts were characterized by TEM, EDS, PXRD, and temperature-programmed oxidation (TPO). It was found that a catalyst containing both Pd and Pt was the most promising, as it had a high activity that did not decline with time. The catalyst containing Pd and Ag was also a promising candidate, but its activity was slightly lower. For PdCo and PdNi, the co-metals formed spinel structures with the alumina support, with the result that the co-metals did not affect the combustion performance of palladium. For PdRh, PdIr, PdCu, and PdAg, the co-metals formed separate particles consisting of the corresponding metal oxide. These catalysts, except PdRh, showed a stable activity. For PdPt and PdAu, the co-metals formed alloys with palladium, and both catalysts showed a stable activity.

Keywords: Palladium; Bimetal; Methane; Catalytic combustion; TEM; EDS; PXRD; TPO

1. Introduction

During the last decades emission standards for combustion-related emissions have become more and more stringent. Hence, it has become increasingly important to find new ways of abating such emissions. Since it is difficult to decrease the pollutants to desirable levels with conventional flame combustion techniques, catalytic combustion has become a highly attractive combustion technique. Catalytic combustion is especially promising for decreasing emissions from the combustion of gaseous fuels such as natural gas or methane in gas turbines [1–3]. The low operation temperature accomplished by this combustion technique results in almost no thermal NO_x and ultra-low emission of CO and hydrocarbons.

The catalysts employed in catalytic combustion for gas turbine applications must be able to ignite the fuel at a temperature as low as 350 °C, which requires very active catalysts. Supported palladium catalysts have an excellent activity for methane oxidation and have therefore been extensively used for catalytic combustion purposes [2,4]. However, palladium catalysts have some drawbacks. At 700–800 °C, depending on the support material and the atmosphere, palladium oxide decomposes into metallic palladium. When the catalyst is cooled, palladium oxide is reformed at a lower temperature than the decomposition temperature. This induces instabilities in the performance of the catalytic combustor. Other disadvantages with palladium catalysts have been observed at temperatures lower than the decomposition temperature. Even though the initial activity is high at these temperatures, the catalyst is not able to maintain the high conversion level during extended time periods; that is, the activity is not stable [5–7]. For this reason, the ignition of the methane will be increasingly difficult. Since palladium-based catalysts have such a high initial activity for methane combustion, it is desirable to improve the stability of the catalytic activity.

One way to increase the stability of the palladium catalysts could be to include a second metal in the catalysts,

* Corresponding author. Fax: +46-8-108579.
E-mail address: katarina.persson@ket.kth.se (K. Persson).

0021-9517/$ – see front matter
doi:10.1016/j.jcat.2005.01.001

forming a bimetallic catalyst. Bimetallic catalysts have been used for several applications other than catalytic combustion and have been established to improve both the activity and selectivity of a great number of reactions [8,9]. The right combination of metals is important for producing the desirable effect. Coq et al. [10] explain the changed behavior of a bimetallic catalyst as an electronic effect, geometry effect, and/or a result of the presence of mixed sites, depending on the co-metal, the metal, and the reaction. However, it is still not fully understood how a bimetallic catalyst works.

Lately, bimetallic catalysts have been given more attention in catalytic combustion applications. Most reports consider methane oxidation over PdPt catalysts. The addition of platinum to a palladium catalyst has been shown to prolong the activity for methane combustion compared with monometallic palladium catalysts [5–7,11–13]. Likewise, PdAg has been reported to maintain its activity over time [5]. Narui et al. [6] attributed the superior combustion stability of PdPt to higher dispersion of supported particles and suppression of particle growth. Whether the activity is higher for the PdPt catalyst compared with the palladium-only catalyst is a debated question. Several authors have also considered the combination of Rh and Pd. However, the opinion regarding the catalytic properties of this catalyst is also divided. Ahlström-Silversand et al. [14] reported positive results for a PdRh catalyst in the temperature range of 300–400 °C, but Ryu et al. [15] and Oh and Mitchell [16] found that rhodium did not noticeably improve the catalytic activity of palladium in methane combustion. Addition of copper to the palladium catalyst has been reported to improve the resistance to sulfur [17].

The purpose of this study was to investigate the catalytic combustion of methane over a range of different compositions of bimetallic catalysts, which all consist of palladium as one of the active components. The co-metals were taken from groups 9–11 in the periodic table. The activity and the ability to maintain a stable activity for methane combustion of the various catalysts have been evaluated. Characterization techniques such as TPO, TEM, EDS, BET, and PXRD have been used to determine the change in morphology, element distribution, and thus properties when a second metal has been incorporated into the palladium catalyst.

2. Experimental

2.1. Catalyst preparation

Different palladium-based catalysts were prepared for this study; they are described in Table 1. All bimetallic catalysts were calculated to have a loading of 470 μmol metal/g catalyst powder, corresponding to the 5 wt% Pd in the reference catalyst (Pd-ref). Furthermore, the bimetallic catalysts were formulated to contain equal molar amounts of palladium and the co-metal, Co, Rh, Ir, Ni, Pt, Cu, Ag, or Au. Three monometallic catalysts, in addition to Pd-ref, have also been prepared, ½ Pd, ½ Pt, and ½ Ni. These catalysts consist of only half the molar amount of metal (235 μmol metal/g catalyst powder), representing the concentration of the corresponding metal in the bimetallic catalysts. The amounts of metals in the catalysts were confirmed by EDS analysis. All catalysts were supported on γ-Al_2O_3 (Condea, PURALOX HP-14/150).

Table 1
The nomenclature and the BET surface area of the different catalysts

Sample	Composition	BET surface area (m^2/g)
Pd-ref	5 wt% Pd//Al_2O_3	102
PdCo	1:1 Pd:Co//Al_2O_3	112
PdRh	1:1 Pd:Rh//Al_2O_3	97
PdIr	1:1 Pd:Ir//Al_2O_3	106
PdNi	1:1 Pd:Ni//Al_2O_3	111
PdPt	1:1 Pd:Pt//Al_2O_3	107
PdCu	1:1 Pd:Cu//Al_2O_3	107
PdAg	1:1 Pd:Ag//Al_2O_3	106
PdAu	1:1 Pd:Au//Al_2O_3	97
½ Ni	Ni//Al_2O_3	–
½ Pd	2.5 wt% Pd//Al_2O_3	–
½ Pt	Pt//Al_2O_3	–

The alumina powder was impregnated with the metal/metals by the incipient wetness technique. The bimetallic catalysts were manufactured by co-impregnation of the two metals, through a mixture of a solution of $Pd(NO_3)_2$ with a solution containing a salt of the co-metal, $Co(NO_3)_2$, $Rh(NO_3)_3$, $IrCl_3$, $Ni(NO_3)_2$, $Pt(NO_3)$, $Cu(NO_3)_2$, $AgNO_3$, or AuCl. The metal solution was dripped onto the alumina and was carefully mixed. This procedure was repeated twice, with a drying step at 300 °C for 4 h in between. The resulting samples were thereafter calcined at 1000 °C for 1 h and cooled at a rate of 20 °C/min to room temperature.

The catalyst powders were mixed with ethanol, and the resulting slurries were ball-milled for 24 h. Cordierite monoliths (400 cpsi, Corning), with ϕ 14 mm and length 10 mm, were then immersed in the slurry, followed by a drying step at 100 °C. This procedure was repeated until 20 wt% catalyst material was fixed on the monolith. The coated monolith was then calcined at 1000 °C for 2 h and cooled at a rate of 2 °C/min to room temperature.

2.2. Characterization

The surface areas of all catalyst powders were measured by nitrogen adsorption at liquid N_2 temperature in a Micromeritics ASAP 2010 instrument. The surface area was determined according to the Brunauer–Emmett–Teller theory. The samples were degassed in vacuum for at least 2 h at 250 °C before analysis.

The crystalline phases in the various catalysts were monitored by powder X-ray diffraction (PXRD), with the use of a Guiner–Hägg camera with a radius of 40 mm. The powder X-ray photographs were evaluated with the program package Scanner System [18] and obtained d-values associated

with crystalline phases in the JCPD database. The diffraction peaks for Pd were used to calculate the mean crystal sizes according to the Scherrer method.

The redox properties of the various catalysts were analyzed by means of temperature-programmed oxidation (TPO). The analyses were carried out with a Micromeritics AutoChem 2910, equipped with a thermal conductivity detector (TCD). A continuous flow of 5 vol% O_2/He was passed over 100 mg calcined catalyst powder. The temperature was increased from 300 to 900 °C at a rate of 10 °C/min, followed by a decrease to 300 °C. The temperature cycle was repeated twice; the results from the second cycle are presented in this paper.

The morphology and chemical composition of fresh catalyst powder were investigated by electron microscopy, combined with equipment for element analysis. The mean compositions of the catalysts were verified in a scanning electron microscope (SEM) (JEOL 820) by energy dispersion X-ray spectroscopy (EDS) (LINK System AN 10000). Composition, element distribution, and morphology on the nanometer scale were studied with a transmission electron microscope (TEM) (JEOL 2000 FX) furnished with EDXS (LINK System AN 10000).

2.3. Activity tests

The catalytic activity for methane combustion over the various catalysts was tested in a conventional tubular reactor, working at atmospheric pressure. The tests were performed on monolith catalysts, described in the previous section. A gas mixture of 1.5 vol% CH_4 in air was fed to the reactor at a space velocity of 250,000 h^{-1}. The temperature was recorded with a thermocouple placed upstream of the monolith. The composition of the product gas was analyzed with an on-line gas chromatograph (GC Varian 3800), equipped with a thermal conductivity detector. Two different activity tests were performed for each catalyst: one in which the temperature was varied continuously and one in which the temperature was varied stepwise. For the tests in which temperature was varied continuously, two consecutive heating and cooling cycles at temperatures from 300 to 950 °C at a rate of 10 °C/min were conducted. The results from the second cycle are used in this study. For the stepwise tests, the experiments were initiated at 475 °C and the temperature was raised stepwise by 50 °C per step to 775 °C. The operating parameters were held constant for 1 h for each temperature.

3. Results

3.1. Powder X-ray diffraction

Diffraction peaks associated with phases in the alumina support material are labeled in the powder X-ray diffractograms, shown in Fig. 1. Because of the high calcination temperature, 1000 °C, the alumina support has changed structure from the initial γ-phase to θ-Al_2O_3 and δ-Al_2O_3. In the cases of PdCo and PdNi, the γ-phase was stabilized and thus remained after heating to 1000 °C.

The PXRD pattern of the as-prepared Pd-ref catalyst shows that palladium appears in crystallites only in its oxide form. A sharp and intense peak representing the (111) reflection of PdO is displayed at $2\theta = 33.81°$. From this and the (111) reflection of the internal silicon standard at $2\theta = 28.44°$, calculation of the mean crystallite size was performed with the Scherrer formula for spherical particles. A value of 40 nm was obtained for PdO in the Pd-ref catalyst. PdO is also observed in PdCo, PdNi, PdCu, PdAg, and PdIr. The mean crystallite sizes of these materials were found to be in the range of 34–50 nm, whereas for the PdIr catalyst a value of 110 nm was determined for PdO.

PXRD patterns of PdCo, PdNi, PdCu, and PdAg did not reveal any crystalline metal oxide phases that could be associated with only the added elements. A similar observation was made for the PdRh material, were only diffraction peaks from the support material were observed, as seen in Fig. 1. However, the PXRD pattern of the PdIr catalyst exhibited, beside γ-Al_2O_3 and PdO, an IrO_2 phase with a mean crystallite size of 190 nm.

The metallic form of Pd was observed in the PXRD patterns of PdPt and PdAu, as solid solutions with Pt or Au. By use of Vegard's law, unit cell parameters of the pure elements, and unit cell parameters determined from the catalysts, the mean composition of the solid solutions was determined to be $Pd_{1-x}Pt_x$, where $x = 0.469$, and $Pd_{1-y}Au_y$, where $y = 0.504$. The mean crystallite sizes of these alloys were calculated to be 35 and 190 nm, respectively.

3.2. Temperature-programmed oxidation

The results of the temperature-programmed oxidation analyses are presented in Fig. 2. The TPO profile of monometallic palladium catalyst, Pd-ref, displays three positive peaks, located close to each other during the heating ramp. The onset temperature for these peaks is 730 °C, and they continue until 900 °C. The peaks arise from the oxygen release occurring when different forms of PdO decompose [19]. PdO does not reoxidize until 620 °C during cooling, when just a single negative peak is detected. The difference between the temperatures of the decomposition and the reoxidation results in a hysteresis. This is typical for supported palladium catalysts.

The palladium content in ½ Pd is equal to the amount of palladium in the bimetallic catalysts. Because of the lower concentration of palladium in ½ Pd, compared with Pd-ref, the intensity of the peaks is lower. Apart from that, the TPO profiles of ½ Pd and Pd-ref are closely matching. As shown in Fig. 2, the TPO profiles of PdCo and PdNi are almost identical to that of ½ Pd. Since ½ Pd corresponds to the palladium content in the bimetallic catalysts, this may indicate that Co and Ni do not affect the oxygen release/uptake in the

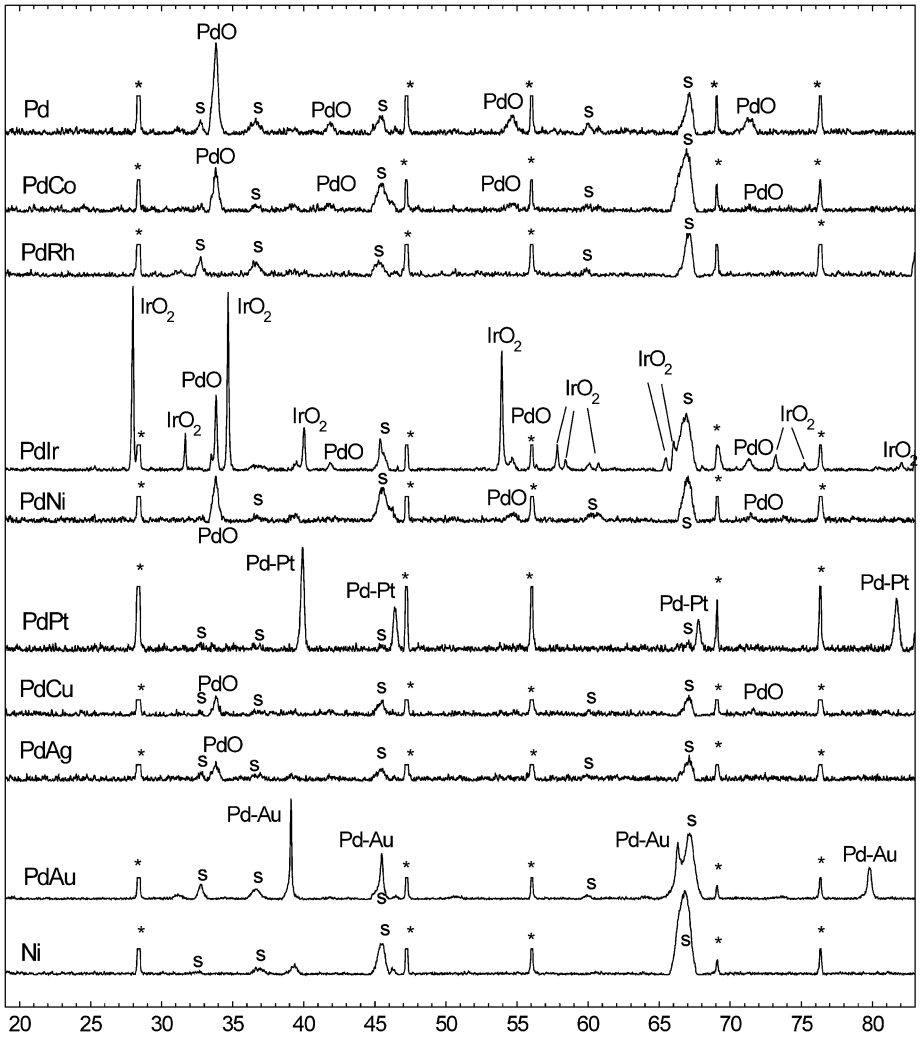

Fig. 1. PXRD patterns of the investigated catalysts. Peaks associated with the alumina support are labelled (s) and the internal standard Si is labelled (*).

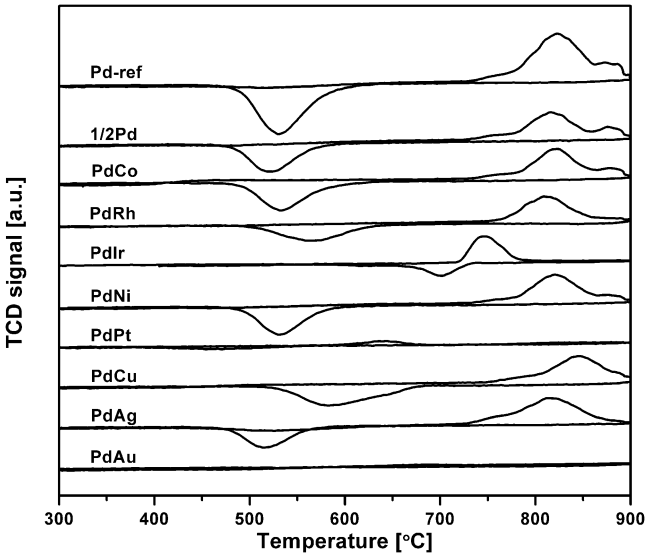

Fig. 2. Temperature-programmed oxidation plots of the various catalysts.

tested temperature range. For PdRh, the first decomposition peak is missing and the intensity is slightly lower than for ½ Pd. Furthermore, the reoxidation peak is slightly shifted to a higher temperature, resulting in smaller hysteresis. PdCu also shows a TPO profile similar to that of ½ Pd, but the reoxidation peak is much broader and initiates at around 685 °C, instead of 620 °C. Furthermore, the decomposition peaks for PdCu appear over a wider range of temperature, and the peaks are not as separated as for the ½ Pd catalyst. PdAg has a TPO profile similar to that of the monometallic palladium catalyst during heating, but during cooling the reoxidation peak is shifted toward a lower temperature, beginning at 575 °C. The TCD signal of PdAg is also slightly lower than that for ½ Pd.

Three catalysts differ markedly from the monometallic palladium catalyst, PdIr, PdPt, and PdAu. PdIr has a sharp decomposition peak with an onset temperature at 710 °C. During cooling, the reoxidation peak appears at clearly higher temperature than for the reference; it initiates at 720 °C and ends at 600 °C. The decomposition and the re-

oxidation peaks appear at almost the same temperature, with just 10 °C difference. For PdPt, only a single peak was observed during heating, and this peak is shifted toward a clearly lower onset temperature at 575 °C. Moreover, the reoxidation peak is shifted downward by 90 °C. The TCD signal detected for this sample was very low, indicating that less oxygen was released from this catalyst than from the reference catalyst. No TCD signal was detected at all for PdAu, indicating that no oxygen release was occurring. The co-metals Ir, Pt, and Ag, supported on Al_2O_3, were separately tested as well, but no TCD signal was detected for any of these metals for the temperature range used in the TPO analysis. Hence, the shifted peaks arise not from the co-metals alone but probably because of interaction between the two metals.

3.3. Transmission electron microscopy

A fragment of the catalyst material of Pd-ref is shown in Figs. 3a–3b. The support material is seen as elongated and partly transparent particles that form large agglomerates in which dark particles are observed. By elemental analysis, these particles were revealed to consist of Pd. The Pd particles were found to be homogeneous and well distributed on the supported material. Some of them are faceted, indicating that they are single crystallites, whereas others seem to be agglomerates of smaller Pd-containing particles. From a number of investigated fragments, the Pd particle sizes were determined to be in the range of 20–80 nm. In the areas between the Pd particles, only aluminum was detected. The ½ Pd sample also exhibited dispersed particles within the same size range, but with a smaller number of particles.

This type of microstructure of particles dispersed on the Al_2O_3 support was also observed in the bimetallic catalyst materials when Co, Ir, Ni, Pt, Cu, Ag, or Au was added as a second element. To describe the element distribution in the bimetallic catalysts, a number of element analyses have been made by spot measurements. This was carried out in two different ways, one with the electron beam focused on a diameter of 20–40 nm on only the Pd particles and the other with the beam diameter size larger than 50 nm on areas of aluminum oxide material without Pd particles. The results from these measurements were then plotted in a graph, with decreasing metal content within each of the two datasets. Three types of element distributions could be distinguished from these analyses of the bimetallic catalysts, as discussed below.

The studies of PdCo and PdNi revealed that Ni and Co were homogeneously and evenly distributed on the support material (see Fig. 4a). TEM micrographs show aluminum oxide with high contrast, whereas the appearance of new particles that could be associated with addition of Co or Ni was not observed. Relative intensities observed in the electron diffraction mode indicate that the structure of the γ-Al_2O_3 particles is stabilized because of formation of the $CoAl_2O_4$ and $NiAl_2O_4$ phases on their surfaces. These phases are probably formed on the surface of the support material. Detectable amounts of Co or Ni could not be observed in the palladium oxide particles.

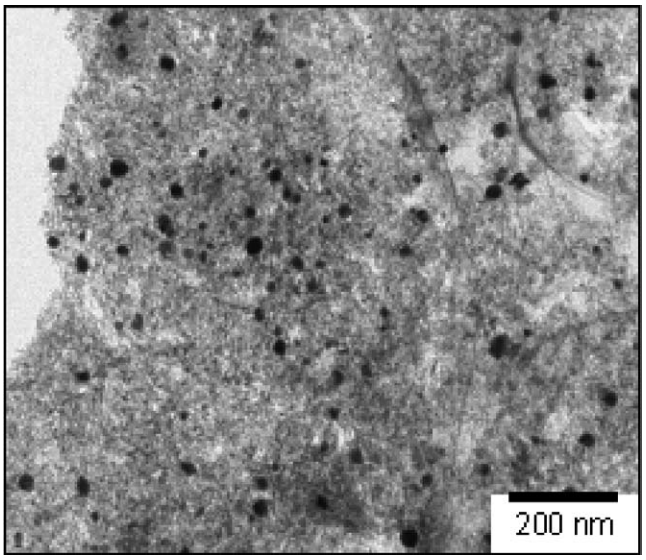

(a)

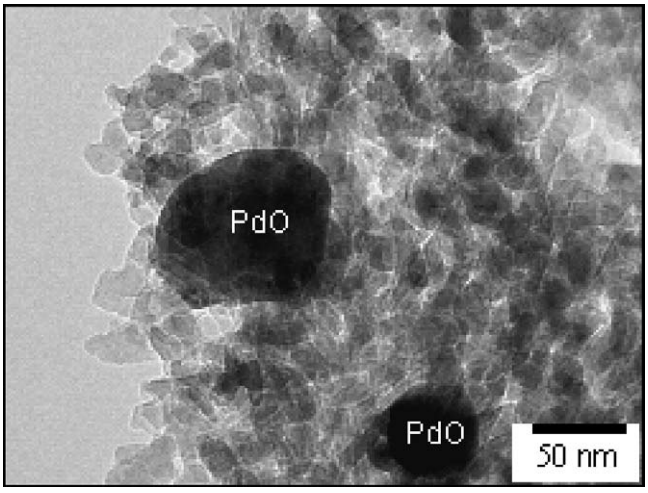

(b)

Fig. 3. TEM images of the Pd-ref catalyst, (a) distribution of PdO particles on alumina and (b) a PdO crystal.

In the PdRh catalyst, palladium oxide particles were observed as agglomerates of Pd particles less than 10 nm across. These agglomerates were 20–40 nm in size and were distributed over the support material in way similar to that of PdO in the Pd-ref catalyst. Rhodium was found to be well distributed all over the alumina support with the appearance of small particles (< 2 nm), but a small number of 2–5-nm particles could be observed around some of the PdO crystals. This was also confirmed by the element distribution shown in Fig. 4b. In the PdCu catalyst, copper was found as particles on the Al_2O_3 support and was enriched near the Pd particles. TEM micrographs reveal that the Cu-containing particles are 1–2 nm in size. This type of particle distribu-

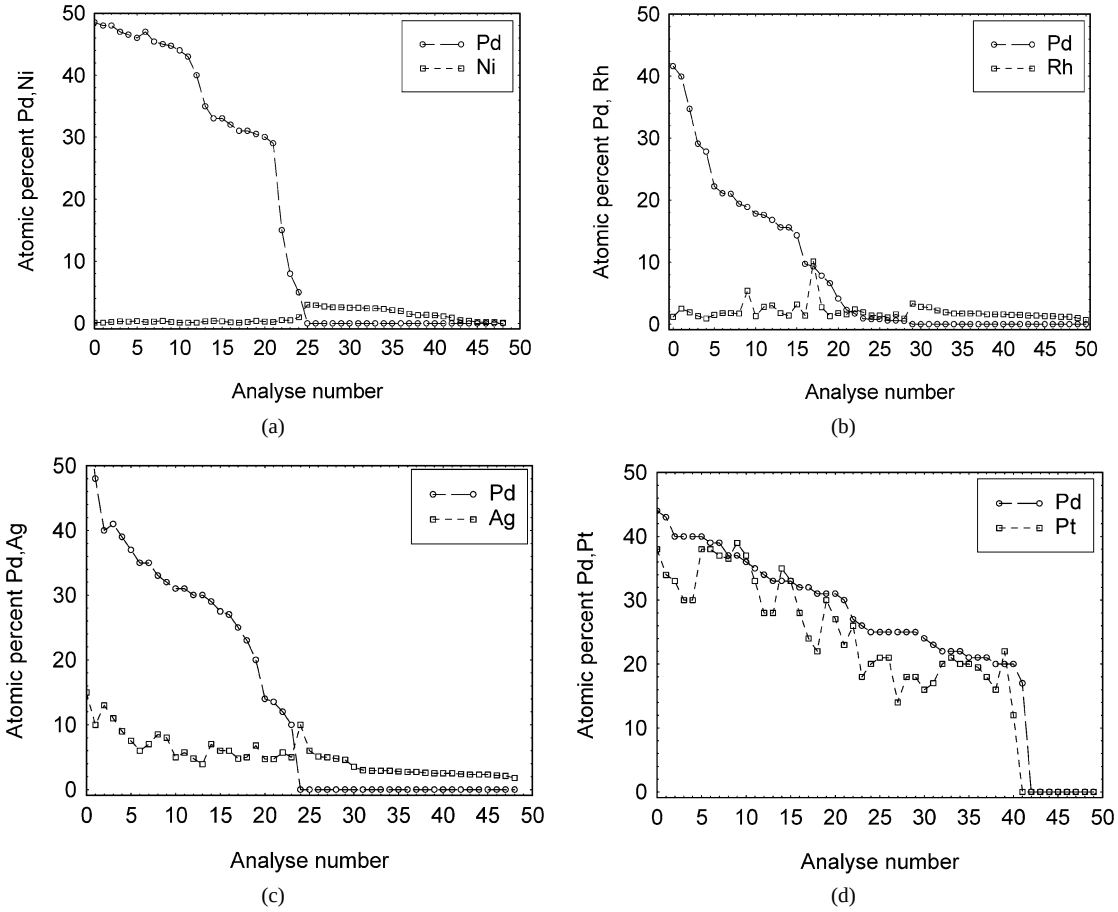

Fig. 4. Spot element analysis obtained by TEM/EDS on particles and Al_2O_3 material in catalysts with the co-metal (a) Ni, (b) Rh, (c) Ag, and (d) Pt.

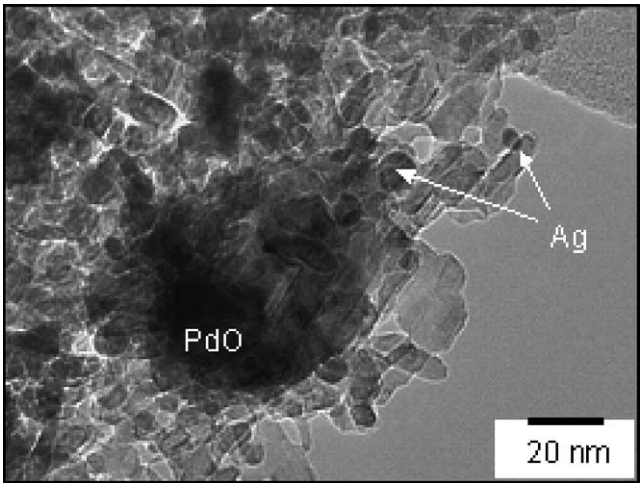

Fig. 5. TEM image of PdO and Ag particles in the PdAg catalyst.

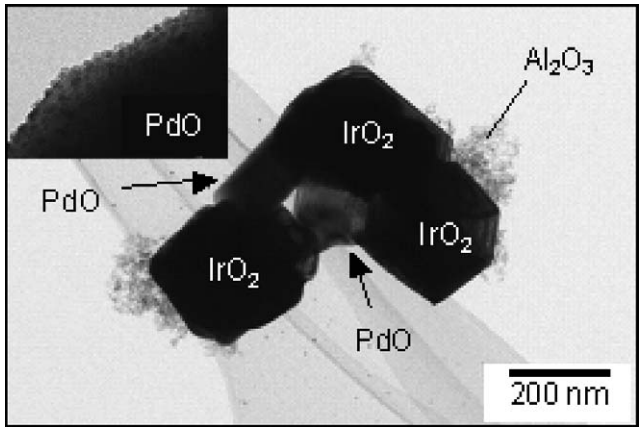

Fig. 6. TEM image of PdO and IrO_2 particles in the PdIr catalyst. Microstructures of surface an PdO crystals shown by insert.

tion was also observed for silver in the PdAg catalyst (see Fig. 4c). The Ag particles were found to be in the range of 1–5 nm, distributed on the support material but also enriched near the PdO crystals (see Fig. 5).

PdIr exhibits a morphology with only metal oxide crystallites larger than 100 nm (100–700 nm), distributed on the alumina support. These crystallites were found to consist of PdO or IrO_2, but not both. An agglomerate of these oxide crystals is shown in Fig. 6. All investigated PdO crystals show faceted crystal surfaces on which small nanometer-sized particles could be observed (see enlarged inset in Fig. 6). The nature of these particles is unclear, as elemental analysis shows only Pd and no other elements, such as Ir or Cl.

For PdAu and PdPt, the distribution of Au and Pt follows the Pd distribution, thus forming metal particles well distrib-

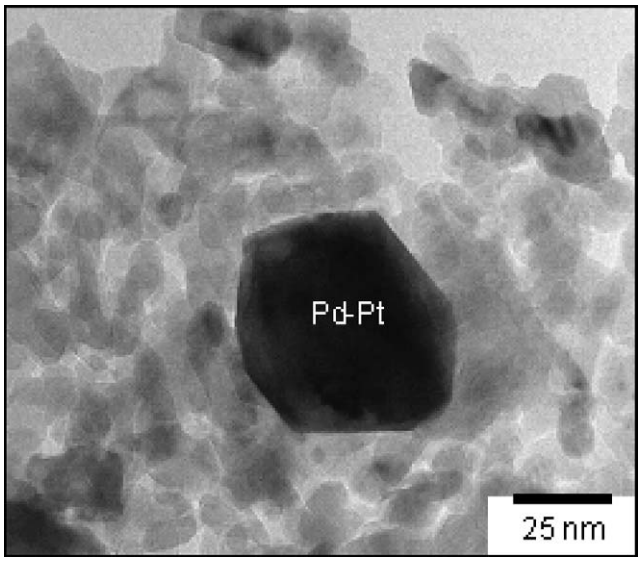

Fig. 7. TEM image of $Pd_{0.5}Pt_{0.5}$ particles in the PdPt catalyst.

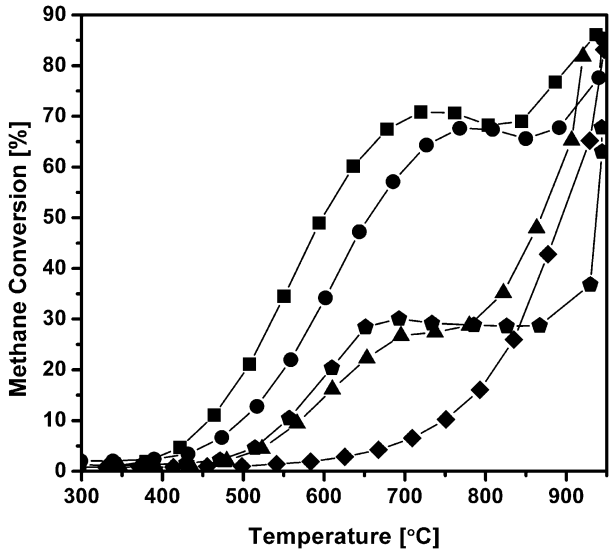

Fig. 8. Activity tests when temperature was varied continuously for Pd-ref (■), PdNi (●), PdPt (▲), PdAg (⬟) and PdCu (◆) during heating ramp.

uted on the alumina, similar to PdO in the Pd-ref catalyst. An alloyed Pd–Pt crystal on alumina is shown in Fig. 7. The composition of the alloyed particles was found by EDS to be very close to the calculated molar ratio 1:1 of PdPt (see Fig. 4d).

3.4. Activity tests with continuously varied temperature

The results from the transient activity tests are displayed in Figs. 8 and 9. Fig. 8 illustrates the combustion behavior observed over the catalyst when the inlet gas was heated from 300 to 950 °C. Pd-ref appears as a typical palladium catalyst, with a dip in conversion starting at around 720 °C during heating. The dip has been explained to be an effect of PdO decomposition into metallic Pd, which is less active for methane combustion [20,21].

For all bimetallic catalysts the effect of PdO decomposition is also observed, except for PdCu. As seen in Fig. 8, PdCu has a very low activity up to 700 °C, after which the methane conversion starts to increase rapidly. PdAg did not show a clear dip at the PdO decomposition temperature, but the methane conversion remained at constant value during the decomposition. A similar behavior was seen for PdPt, but the temperature region where PdO decomposes was much smaller and the conversion started to rise at lower temperature than for PdAg. The drop in conversion due to PdO decomposition was shifted to a higher temperature for PdNi. PdCo and PdRh showed behavior similar to that of PdNi and therefore are not shown in the figure. The reoxidation of palladium during the cooling ramp (not shown in the figure) occurs at a higher temperature for PdRh, PdAg, and PdIr than for the reference catalyst.

The temperatures required to reach 10, 30, and 50% methane conversion (T_{10}, T_{30}, and T_{50}) over the catalysts are shown in Fig. 9. Among the bimetallic catalysts, PdNi was the most active, but, as previously discussed, this catalysts

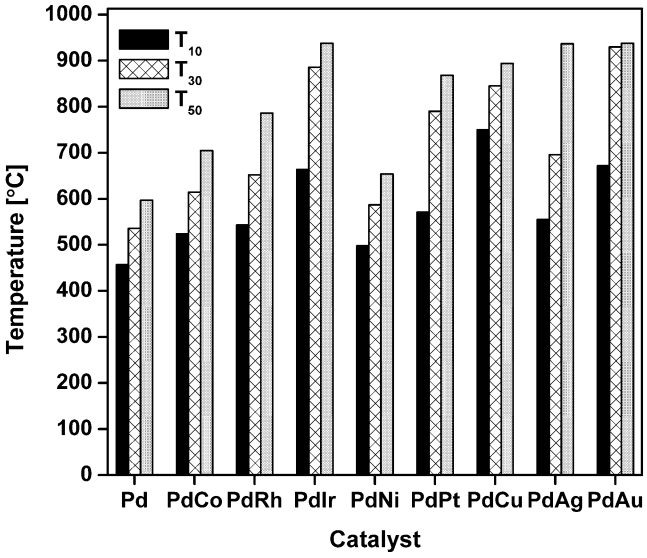

Fig. 9. The temperature required for 10, 30, and 50% methane conversion (T_{10}, T_{30}, and T_{50}) of the catalysts.

has an activity similar to that of ½ Pd. PdCo was approximately as active as PdNi. PdIr and PdAu, on the other hand, display a poor activity for methane combustion.

3.5. Activity tests with temperature varied stepwise

The results from the activity tests conducted when the temperature was varied stepwise are presented in Figs. 10–14. In these activity tests, the stability of the activity was studied at different temperatures. The monometallic palladium catalyst, Pd-ref, is used as a reference catalyst and is therefore displayed in all of Figs. 10–12. As illustrated in these figures, Pd-ref initially has a high activity, but the methane conversion decreases rapidly with time on stream.

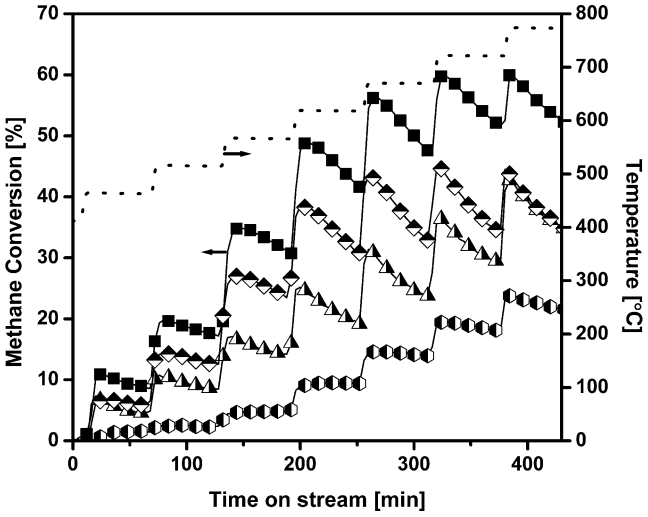

Fig. 10. Activity tests when temperature was varied stepwise for Pd-ref (■), PdCo (◆), PdRh (▲) and PdIr (◐). The dotted line represents the inlet temperature of the catalysts.

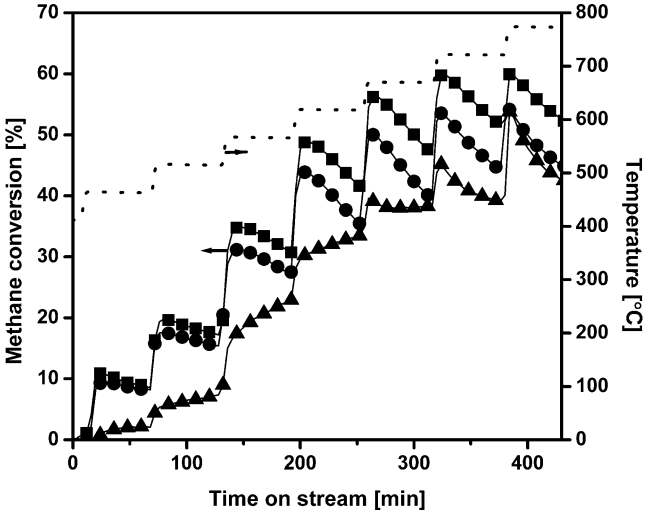

Fig. 11. Activity tests when temperature was varied stepwise for Pd-ref (■), PdNi (●) and PdPt (▲). The dotted line represents the inlet temperature of the catalysts.

The methane conversion even decreases for Pd-ref at such a low temperature as 475 °C.

Fig. 10 shows the results of the activity tests for catalysts consisting of co-metals from group 9 in the periodic table. A large variation in methane conversion between the catalysts is observed. Both PdCo and PdRh show unstable activity similar to that of Pd-ref. PdIr, on the other hand, achieves a stable activity without any decrease in conversion. However, the activity of PdIr is fairly low.

Fig. 11 illustrates the methane conversion over the catalysts consisting of co-metals from group 10 in the periodic table. PdNi initially obtains an excellent methane conversion, close to the values achieved for Pd-ref. However, the activity of PdNi is unstable, and like that of the reference catalyst, drops with time on stream for all temperature

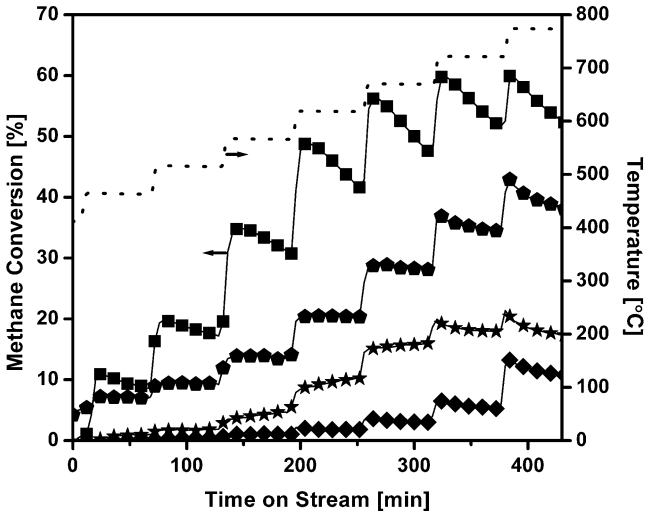

Fig. 12. Activity tests when temperature was varied stepwise for Pd-ref (■), PdCu (◆), PdAg (⬟), and PdAu (★). The dotted line represents the inlet temperature of the catalysts.

steps. PdPt is, in contrast, much more stable for temperatures below 675 °C, before the PdO decomposition begins. For temperatures above the PdO decomposition, the methane conversion decreases for this catalyst as well. PdPt obtains low activity of methane conversion for the two first temperature steps, at 475 and 525 °C, respectively. For the following steps, the activity actually increases with time on stream.

Fig. 12 illustrates the methane conversion over the catalysts consisting of co-metals from group 11 in the periodic table. The range of methane conversion of the various catalysts is large. It is interesting that all catalysts from this group achieve a stable activity. However, PdCu displays a very poor conversion, and it is difficult to decide whether the activity is stable. PdAg obtains the highest activity of the catalysts from group 10, although its activity is not as good as that of PdPt shown in Fig. 11. However, the methane conversion of PdAg is constant for 50 °C higher temperature than for PdPt, that is, up to 725 °C. PdAu exhibits low activity for all temperature steps, although its conversion is higher than for PdCu. Common for all tested catalysts, it appears that the methane combustion is lower for the stable catalysts compared with the unstable ones.

To study the effect of the co-metals, ½ Pd, ½ Ni, and ½ Pt have been considered; the results are presented in Figs. 13 and 14. The two catalysts ½ Pd and ½ Ni correspond to the contents of palladium and nickel, respectively, in PdNi. Analogously, ½ Pd and ½ Pt correspond to the palladium and platinum contents in PdPt. Fig. 13 shows that ½ Ni does not have any activity for methane combustion at all, regardless of temperature. ½ Pd, however, obtains the same activity as PdNi. PdNi-additional is here defined as the sum of methane conversion of ½ Ni and ½ Pd. Since ½ Ni does not show any activity, PdNi-additional is the same as ½ Pd. Moreover, PdNi-additional overlaps the curve representing the methane conversion over PdNi. Therefore, the palladium in PdNi appears to be unaffected by the presence

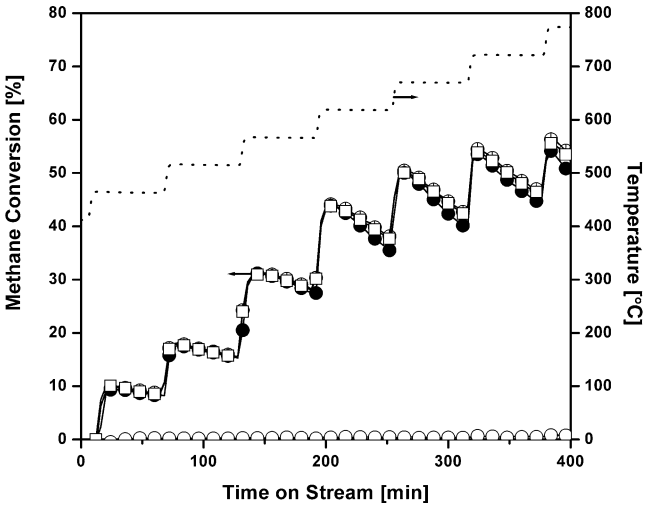

Fig. 13. Activity tests when temperature was varied stepwise for ½ Ni (○), ½ Pd (□), PdNi-additional (⊕), and PdNi (●). The dotted line represents the inlet temperature of the catalysts.

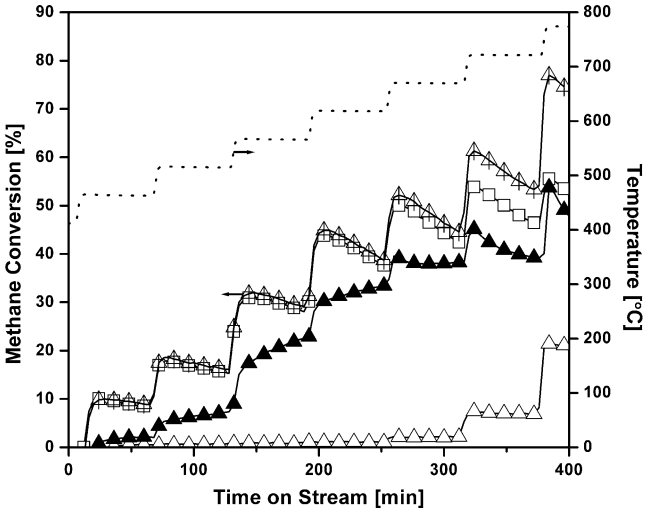

Fig. 14. Activity tests when temperature was varied stepwise for ½ Pt (△), ½ Pd (□), PdPt-additional (◭), and PdPt (▲). The dotted line represents the inlet temperature of the catalysts.

of nickel and Ni and Pd are probably not in close contact. Hence, the addition of nickel to a palladium catalyst has no beneficial effect on the activity. Fig. 14 shows that ½ Pt gains activity first at 675 °C and reaches a methane conversion of 21% at 775 °C. The combustion over ½ Pt is much more stable than that over ½ Pd. However, the initial activity of ½ Pd is superior. Its activity is even higher than for PdPt. PdPt-additional, the sum of the methane conversion of ½ Pd and ½ Pt, is not a direct superimposition of PdPt, indicating the existence of a close interaction. The rapid increase in methane conversion at 775 °C follows ½ Pt.

4. Discussion

4.1. Catalyst materials

In the catalyst materials that have been used in this study of methane conversion, the palladium appears as particles of oxides or alloys. Because of the chemistry and distribution of the added co-metals, the bimetallic catalysts can be divided into three types, depending on how the co-metal interacts with the support and/or the palladium (see Table 2).

In the first group of catalysts, the co-metal appears to react with the alumina support to produce a spinel structure. This has been shown for PdCo and PdNi. This is in accordance with the TPO profiles of PdNi and PdCo that are similar to the profile of ½ Pd, which represents the amount of Pd in the bimetallic catalysts. This is also strengthened by the TEM results, where both Co and Ni are well spread over the alumina. Neither of the catalysts has been shown to produce separate particles or to be in close contact with the Pd particles. However, no spinel phase was observed in the PXRD diffractograms, probably because the size of the spinel particles was below the detection limits of the instrument. It is interesting that the alumina maintains its γ-phase despite the high calcination temperature at 1000 °C, and it may therefore be a good support material.

The second group of bimetallic catalysts have been seen by TEM to produce separate particles of the co-metals. For this group, effects on the PdO decomposition and reoxidation processes during TPO measurements were seen, which were due to morphology and interaction between the palladium and the co-metal. The decomposition temperatures of PdRh, PdCu, and PdAg were similar to that of PdO, whereas Rh_2O_3 and CuO increased the reoxidation temperature and Ag_2O decreased this temperature.

Table 2
Types of catalyst materials that have been investigated and description of the materials

Catalyst type	Catalyst	Description of interaction of the co-metal with the palladium or alumina support
$PdO//MeAl_2O_4/Al_2O_3$	PdCo	20–40 nm PdO particles on cobalt spinel–alumina support
	PdNi	20–40 nm PdO particles on nickel spinel–alumina support
$PdO/MeO//Al_2O_3$	PdRh	1–5 nm agglomerated PdO particles and < 2 nm Rh_2O_3 particles on alumina support
	PdIr	80–600 nm PdO and 80–200 nm IrO_2 crystals on alumina support
	PdCu	34–50 nm PdO particles and 1–5 nm CuO particles on alumina support
	PdAg	34–50 nm PdO particles and 1–5 nm Ag_2O particles on alumina support
$Pd–Me//Al_2O_3$	PdPt	Pd–Pt alloy with particle size of 35 nm on alumina support
	PdAu	Pd–Au alloy with particle size of 190 nm on alumina support

The PdIr catalyst exhibits a TPO curve that clearly indicates that Ir affects the PdO. This is surprising, as the PXRD and TEM studies show that Pd and Ir appear as large and separated oxide particles. However, micrographs of the PdO crystals (see Fig. 6) reveal that the surfaces of the crystals are covered with 1–2-nm particles. It is unclear from the TEM/EDS studies whether these particles consist of metallic Pd, Ir, a Pd–Ir alloy, or any oxide compound. Still, it is obvious that these particles are in good contact with the large PdO crystals and are responsible for the change in the oxygen release/uptake behavior of PdO. Thus, the surface particles can be assumed to be in metallic form and to consist of Ir or Pd–Ir alloy, and not of Pd, as Pd will normally form PdO under these conditions.

In the third group of bimetallic catalysts, PdPt and PdAu, the co-metals alloy with palladium. The alloy formation is supported by the TEM analysis, where no co-metal was found on the alumina support but only close to the palladium. In the PXRD diffractograms of both PdPt and PdAu, a sharp peak is located around the position of metallic Pd(111). However, these peaks are shifted toward the peaks representing the metallic form of the co-metals, indicating an alloy.

The alloyed catalyst $Pd_{1-y}Au_y$, with metal composition $y = 0.504$, shows no pronounced TPO profile. Venezia et al. [22] have also reported an alloying between Au and Pd. The study showed that the amount of PdO decreases with increasing Au. This is in good agreement with our results, where our equimolar PdAu catalyst showed no oxygen release/uptake in the TPO experiments. For all other tested catalysts, some PdO must be present, since at least one TPO peak was detected, even though some of the co-metals affect the location of the peak.

4.2. Activity and stability under conditions of methane conversion

In the first group of bimetallic catalysts, comprising the catalysts PdCo and PdNi, the co-metal is probably reacting with the alumina support to form a spinel phase. The activity of this group is as unstable as the monometallic palladium catalyst. This may be explained by the co-metal being found in the spinel phase and not interacting with the palladium particles; hence the palladium particles will behave as the monometallic palladium catalyst does. This is supported by the results in Fig. 13, where the addition of Ni to the palladium catalyst does not affect the total methane conversion. The Co and Ni spinels have been reported to have poor activity for methane combustion [23,24]. The methane conversion of PdCo is slightly lower than the conversion of ½ Pd. It is not clear, at present, what causes the lower activity.

In the second group of bimetallic catalysts, PdRh, PdIr, PdCu, and PdAg, the co-metals oxidize and produce separate particles. This is a complex group, in which the stability of the activity appears to be dependent on how close the co-metal is to the palladium particles. PdRh showed unstable activity. The reason for this may be that Rh is not as enriched close to the palladium particles as for the other catalysts in this group, but is located more on the alumina. The instability may also be deduced by the small particle size. Contrary to the results presented in this paper, the literature regarding rhodium-containing palladium catalysts suggests that the combustion is fairly stable [7,12]. However, the presented conversion is poor, and it is difficult to state whether the catalyst is stable. Other researchers have also observed low activity for rhodium-based palladium catalysts [15,16].

For PdIr, the activity is stable but low. This result is the opposite of what Nomura et al. [12] have shown. The low activity of PdIr may arise from the large particle size. The precursor, $IrCl_3$, may also affect the combustion activity, since chlorine has been shown to poison palladium easily [25]. However, this is not the case, because of the high calcination temperature.

For PdCu and PdAg, the co-metals may be found close to the palladium particles. Both of these catalysts are stable, even though the activity of PdCu is low. The poor activity of PdCu may be explained by CuO partly covering the palladium particles. This is in line with the results from the activity test presented in Fig. 8, where the activity curve differs from the palladium profile, with no drop in conversion due to PdO decomposition. Reyes et al. [17] reported that copper itself has poor combustion activity for methane, but that the activity of PdCu is slightly better than that of copper but not as good as that of monometallic palladium.

As discussed previously, silver particles are located on the palladium particles and on the alumina support. Since the Ag_2O is in close contact with the palladium particles, but does not cover the particles completely, the PdAg catalyst may reach a higher activity than PdCu. The differences in activity of this group may also arise from the individual activity of the co-metals alone.

The third group represents co-metals that alloy with palladium. The catalysts in this group, comprising PdPt and PdAu, present a stable activity. The higher stability of catalysts consisting of both palladium and platinum has been reporter by other researchers as well [5–7,11–13]. Whether these catalysts are more or less active than monometallic palladium catalysts is a debated question. A range of results can be found in the literature, obtained under various conditions. In this study the comparison between the catalysts was made with the molar amount of precious metals kept constant. It was found that the activity of PdPt was lower than that of the monometallic Pd catalyst. The methane conversion increases, on the other hand, instead of decreasing with time. This may be due to formation of PdO on the catalyst during operation, but further studies are required to verify this. If this is the case, the PdPt catalyst may become very active after a while. As shown in Fig. 14, the effect of Pt on the methane combustion is not a superposition of ½ Pt on ½ Pd, which indicates that palladium and platinum are closely interacting.

The difference in activity between PdPt and PdAu may be explained by the difference in PdO content. This is in line with the results from the TPO analysis, where no signal for oxygen release was observed for PdAu, but a small peak was observed for PdPt. Since the PdO is claimed to be more active than its metallic phase in this temperature range [20,26], the lower oxide content will reflect on the activity. The low activity may also be due to the chlorine precursor used for the gold catalyst and/or the larger particle size of PdAu. Low activities of PdAu catalysts have also been reported by others [14,27].

The present study shows that it may be possible to stabilize the activity of palladium catalysts with the addition of certain metals. However, further testing is needed to verify the long-term stability. The two most promising candidates tested in this study are PdPt and PdAg. Both catalysts obtained stable activity, but the level of activity is higher for PdPt. Other metal combinations tested in this study display either poor methane conversion or unstable activity.

Ciuparu et al. [4] have reported on the large sensitivity to water inhibition of monometallic palladium catalysts due to $Pd(OH)_2$ formation. This is important, since water is one of the reaction products in combustion of methane. Unpublished results obtained at our laboratory have shown that water inhibition during combustion may be an essential factor for obtaining a stable activity over palladium-based catalysts. Furthermore, the bimetallic PdPt is less sensitive to water in the process steam compared with monometallic palladium catalysts. According to Ishihara et al. [28], metal oxides added to a palladium catalyst provide oxygen to the Pd. Ciuparu et al. [29] have suggested that the support materials with high oxygen mobility, such as ZrO_2, can improve the resistance to water inhibition of monometallic palladium catalysts. The reason for this may be that the oxygen from the support and the water compete for the same active sites. This may also be the case for metal oxides. Hence, the oxygen from the metal oxide may compete with the water located on the palladium. However, for this to occur the oxide and the palladium particles probably must be in close contact. When an alloy is present the formation of $Pd(OH)_2$ is also probably minimized.

Another explanation for the stable activity of some of the bimetallic catalysts may be the suppression of the change in the PdO structure during combustion, as reported by Groppi et al. [19,30] for monometallic palladium catalysts. According to Narui et al. [6], the suppression of particle growth by the platinum may also explain the more stable activity over the bimetallic PdPt catalyst.

5. Conclusions

To stabilize the activity over palladium catalysts during methane combustion, a series of eight different co-metals has been tested. The results show that it may be possible to stabilize the activity over the palladium catalyst with the addition of certain metals. The conclusions are as follows:

- Three different cases have been observed for the behavior of the co-metals: the co-metal reacts with the alumina support to form a spinel phase, the co-metal forms separate particles, or the co-metal alloys with Pd.
- The activity of the catalysts decreased in the following order according to the T_{10} values obtained when the temperature was varied continuously: Pd > PdNi > PdCo > PdRh > PdAg > PdPt > PdIr > PdAu > PdCu. However, the PdPt catalysts obtained a higher activity in the activity tests in which the temperatures were kept constant.
- Even though the activity is initially high, the activity may decrease with time. When both the stability and the level of activity for methane combustion are considered, PdPt is the most promising of the catalysts tested in this study for methane combustion. PdAg is also very stable, but it is slightly less active than PdPt.
- Co-metals forming a spinel structure (PdCo and PdNi) do not improve the stability of the activity of palladium catalysts. However, the spinel structure appears to improve the thermal stability of the support material. Co-metals forming separate particles (PdRh, PdIr, PdCu, and PdAg) may improve the stability, depending on whether the co-metals are in close contact with Pd. Co-metals forming an alloy with Pd (PdPt and PdAu) do obtain stable activity.

Acknowledgments

The Swedish Energy Agency is acknowledged for financially supporting this work. Thanks are due to Condea GmbH for providing the alumina support.

References

[1] W.C. Pfefferle, J. Energy 2 (1978) 142.
[2] E.M. Johansson, D. Papadias, P.O. Thevenin, A.G. Ersson, R. Gabrielsson, P.G. Menon, P.H. Björnbom, S.G. Järås, in: J.J. Spivey (Ed.), Catalysis—Specialists Periodical Reports, vol. 14, Royal Society of Chemistry, Cambridge, 1999, p. 183.
[3] M.F.M. Zwinkels, S.G. Järås, P.G. Menon, T.A. Griffin, Catal. Rev. Sci. Eng. 35 (1993) 319.
[4] D. Ciuparu, M.R. Lyubovsky, E. Altman, L.D. Pfefferle, A. Datye, Catal. Rev. 44 (2002) 593.
[5] R.A. Della Betta, K. Tsurumi, T. Shoji, R.L. Garten, US Patent 5405 260 (1995), to Catalytica Inc. and Tanaka Kikinzoku Kogyo K.K.
[6] K. Narui, H. Yata, K. Furuta, A. Nishida, Y. Kohtoku, T. Matsuzaki, Appl. Catal. A 179 (1999) 165.
[7] A. Ersson, H. Kušar, R. Carroni, T. Griffin, S. Järås, Catal. Today 83 (2003) 265.
[8] V. Ponec, Appl. Catal. A 222 (2001) 31.
[9] B. Pawelec, R. Mariscal, R.M. Navarro, S. van Bokhorst, S. Rojas, J.L.G. Fierro, Appl. Catal. A 225 (2002) 223.
[10] B. Coq, F. Figueras, J. Mol. Catal. A 173 (2001) 117.
[11] H. Yamamoto, H. Uchida, Catal. Today 45 (1998) 147.

[12] K. Nomura, K. Noro, Y. Nakamura, Y. Yazawa, H. Yoshida, A. Satsuma, T. Hattori, Catal. Lett. 53 (1998) 167.
[13] Y. Ozawa, Y. Tochihara, A. Watanabe, M. Nagai, S. Omi, Appl. Catal. A 259 (2004) 1.
[14] A.F. Ahlström-Silversand, C.U.I. Odenbrand, Appl. Catal. A 153 (1997) 157.
[15] C.K. Ryu, M.W. Ryoo, I.S. Ryu, S.K. Kang, Catal. Today 47 (1999) 141.
[16] S.H. Oh, P.J. Mitchell, Appl. Catal. B 5 (1994) 165.
[17] P. Reyes, A. Figueroa, G. Pecchi, J.L.G. Fierro, Catal. Today 62 (2000) 209.
[18] K.E. Johansson, T. Palm, P.E. Werner, J. Phys. Sci. Instrum. 13 (1980) 1289.
[19] G. Groppi, C. Cristiani, L. Lietti, P. Forzatti, in: A. Corma, F.V. Melo, S. Mendioroz, J.L.G. Fierro (Eds.), Studies in Surface Science and Catalysis, vol. 130, Elsevier, Amsterdam, 2000, p. 3801.
[20] R.J. Farrauto, M.C. Hobson, T. Kennelly, E.M. Waterman, Appl. Catal. A 81 (1992) 227.
[21] J.G. McCarty, Catal. Today 26 (1995) 283.
[22] A.M. Venezia, V. La Parola, V. Nicolì, G. Deganello, J. Catal. 212 (2002) 56.
[23] E. Garbowski, M. Guenin, M. Marion, M. Primet, Appl. Catal. 64 (1990) 209.
[24] Y. Lu, Y. Liu, S. Shen, J. Catal. 177 (1998) 386.
[25] D. Roth, P. Gélin, M. Primet, E. Tena, Appl. Catal. A 203 (2000) 37.
[26] R. Burch, F.J. Urbano, Appl. Catal. A 124 (1995) 121.
[27] S. Miao, Y. Deng, Appl. Catal. B 31 (2001) L1.
[28] T. Ishihara, H. Shigematsu, Y. Abe, Y. Takita, Chem. Lett. (1993) 407.
[29] D. Ciuparu, E. Perkins, L. Pfefferle, Appl. Catal. A 263 (2004) 145.
[30] G. Groppi, G. Artioli, C. Cristiani, L. Lietti, P. Forzatti, in: E. Iglesia, J.J. Spivey, T.H. Fleisch (Eds.), Studies in Surface Science and Catalysis, vol. 136, Elsevier, Amsterdam, 2001, p. 345.